Facile preparation of $Zn_2V_2O_7$-VO_2 composite films with enhanced thermochromic properties for smart windows

Yongqiang Zhang [a,#], Bin Li [a,#], Zhe Wang [a], Shouqin Tian*[,a], Baoshun Liu [a], Xiujian Zhao [a], Neng Li*[,a], Gopinathan Sankar [b], Shifeng Wang [c]

[a] State Key Laboratory of Silicate Materials for Architectures, Wuhan University of Technology (WUT), No. 122, Luoshi Road, Wuhan 430070, P. R. China

[b] Department of Chemistry, Materials Chemistry Centre, University College London, 20 Gordon St., London WC1H 0AJ, UK

[c] Department of Physics, Innovation Center of Materials for Energy and Environment Technologies, College of Science, Tibet University, Lhasa 850000, China

[#]The authors contributed equally.

*Corresponding author. Tel.: +86-027-87652553; Fax: +86-027-87883743.

*E-mail address: tiansq@whut.edu.cn (S. Tian), lineng@whut.edu.cn (N. Li)

ABSTRACT:

Usually, VO_2 film prepared by magnetron sputtering method exhibits good durability and excellent solar modulation efficiency (ΔT_{sol}). However, its undesirable low temperature luminous transmittance (T_{lum}) limits its application in the smart windows since the dense film composed of VO_2 nanocrystals with narrow band gap can absorb more visible light. In this work, $Zn_2V_2O_7$-VO_2 composite film was deposited on quartz glass by a facile magnetron sputtering method followed by post annealing at 450 ºC, in which transparent $Zn_2V_2O_7$ aimed to improve the optical performance. The composite film showed an enhanced thermochromic performance with ΔT_{sol} of 11.5%, T_{lum} of 49.0% and phase transition temperature (T_c) of 43.8 ºC compared with pure VO_2 film (T_{lum} = 34.1%, ΔT_{sol} = 10.9%, T_c = 49.2 ºC). This was probably attributed to the formation and uniform distribution of $Zn_2V_2O_7$ in the composite film which could widen the optical band gap, leading to the improvement in the optical properties. The interface between $Zn_2V_2O_7$ and VO_2 could produce interfacial stress to reduce the phase transition temperature. Therefore, this work can provide a facile way to improve the thermochromic performance of VO_2 based films and promote their application in the field of energy-saving glass.

KEYWORD: $Zn_2V_2O_7$-VO_2 composite film; magnetron sputtering; solar modulation efficiency; luminous transmittance; phase transition temperature;

INTRODUCTION

Recently, VO_2 has been considered as the most promising material for energy-saving smart windows due to its unique thermochromic properties.[1-3] Bulk VO_2 undergoes a reversible phase transition from monoclinic phase (VO_2(M)) to rutile phase (VO_2(R)) at 68 ºC,[4] accompanied by large changes in optical properties.[5] The phase transition temperature of VO_2 is called as the critical temperature (T_c).[6] When the temperature is lower than T_c, VO_2 based coatings are transparent to near infrared (NIR) light; while the temperature is higher than T_c, they could reflect most of the NIR light, thereby reducing the transmittance of NIR (T_{NIR}) light.[7] With the ability of modulating (T_{NIR}) in response to the ambient temperature, ideally, VO_2 coatings based smart windows could keep indoor warm in cold winter while cool in hot summer to reduce energy consumption.[6]

There are many methods to prepare VO_2 thin films on the glass substrates, including magnetron sputtering,[7] pulsed laser deposition,[8] hydrothermal methods,[9] vacuum evaporation,[10] chemical vapor deposition,[11] and ion implantation.[12] In these methods, magnetron sputtering is widely used since it demonstrated strengths of high repeatability, suitability for mass production and preparing coatings with uniform density, good durability, excellent solar modulation efficiency.[5] However, the pure VO_2 film prepared by magnetron sputtering not only presented low but also showed a high phase transition temperature,[13-14] since the VO_2 nanocrystals with narrow band gap of 0.67 eV,[15] which could absorb visible light thus lowering luminous transmittance. In order to solve the above problems, many methods have been adopted. The phase transition temperature of the film could be reduced by element doping. The most typical element is W. The incorporation of W into VO_2 crystals can reduce the phase transition temperature of VO_2 film by 15-40 ºC /at% depending on the preparation method, however, the solar modulation efficiency and the luminous transmittance of the film would be deteriorated equally.[16-19] The incorporation of Mg can also reduce the phase transition temperature of the VO_2 film and improve luminous transmittance, but the solar modulation efficiency of the film is reduced.[20]

Other elements such as Nb^{5+}, Mo^{6+} can also reduce the phase transition temperature of the films, but affect the solar modulation efficiency and the luminous transmittance.[19,21] In addition, there are other methods that can also reduce the phase transition temperature of the film by precisely controlling the oxygen partial pressure and the atmosphere for annealing, while both failed to investigate the luminous transmittance and solar modulation efficiency.[22,23] The weak luminous transmittance of VO_2 films prepared by magnetron sputtering is mainly caused by inherent absorption and reflection. The addition of anti-reflection layer on the surface of VO_2 film can increase the optical properties of the film.[24-26] By preparing VO_2/AZO, TiO_2(R)/VO_2(M)/TiO_2(A), TiO_2/VO_2/TiO_2/VO_2/TiO_2 and other multilayer film structures, the luminous transmittance could also be increased,[27-29] but these methods had little effects on the phase transition temperature of the VO_2 film. Therefore, it is of great significance to fabricate VO_2-based film with reduced phase transition temperature, good luminous transmittance and excellent solar modulation efficiency.

In this work, $Zn_2V_2O_7$ with wide band gap was introduced into the VO_2 film to obtain a single-layer composite film by magnetron co-sputtering zinc oxide and vanadium targets followed by post annealing.[30,31] The obtained uniform $Zn_2V_2O_7$-VO_2 composite film exhibits good T_{lum} of 49.0%, suitable ΔT_{sol} of 11.5% and reduced T_c of 43.8 ºC compared with pure VO_2 film ($T_{lum\text{-}L}$ = 34.1%, ΔT_{sol} = 10.9%, T_c = 49.2 ºC). Optimization of thermochromic performance is probably attributed to the dispersion structure of $Zn_2V_2O_7$ nanograins in the composite film. In addition, the reduced phase transition temperature is probably caused by interfacial stress produced by the heterojunction between VO_2 and $Zn_2V_2O_7$ grains. It is believed that the proposed universal approach will further promote the development of the practical smart windows in energy-saving buildings.

EXPERIMENTAL METHODS

Preparation of $Zn_2V_2O_7$-VO_2 composite film. The $Zn_2V_2O_7$-VO_2 composite film was fabricated on 25×25×1 mm quartz glass substrate via a magnetron co-sputtering system and post annealing. V target (99.95%) and ZnO (99.99%) target were used for

co-deposition. Before sputtering, the vacuum chamber was evacuated to 3.0×10^{-3} Pa. Then, Ar (99.99%) was introduced into the chamber and the gas flow rate was fixed at 200 sccm. During the deposition, keeping the substrate at ambient temperature. ZnO-V composite films were deposited through direct current magnetron sputtering of V targets and radio frequency magnetron sputtering of ZnO targets simultaneously at identical power of 75 W. The vanadium target was continuously sputtered for 16 min, while the ZnO target was intermittently co-sputtered at 4-minute intervals for 1 min starting at 1.5 min after vanadium sputtering began and sputtering time lasted 4 min in total. Finally, the post-annealing process was performed to transfer ZnO-V composite films to $Zn_2V_2O_7$-VO_2 composite films. In detail, ZnO-V composite films was annealing at 450 ºC for 1 h, prior to ramping up temperature to the annealing temperature at the ramp rate of 5 ºC/min, the air pressure in the tube furnace was controlled at 1100 Pa promising to oxidize V to VO_2. The $Zn_2V_2O_7$-VO_2 composite films was obtained after furnace naturally cool down. It is worth noting that post annealing was necessary for preparing the $Zn_2V_2O_7$ from reaction between VO_2 and ZnO, since the reaction took time and required high enough temperature, even though that would extend production time compared with the magnetron sputtering method that in-site growth VO_2 under O_2 flow. The whole fabrication process of the composite film was illustrated in detail in Figure 1. For comparison, $Zn_2V_2O_7$-VO_2 composite films with various total ZnO sputtering duration (2min, 6min) and in particular pure VO_2 film (0 min), $Zn_2V_2O_7$ (16 min) film denoted as VZ2, VZ6, V and VZ16 separately were also prepared to justify the effect of V/Zn ratio on thermochromic properties of composite films by the same method, and the detailed preparation process was described in Figure S1. The specific parameters were summarized in Table S1.

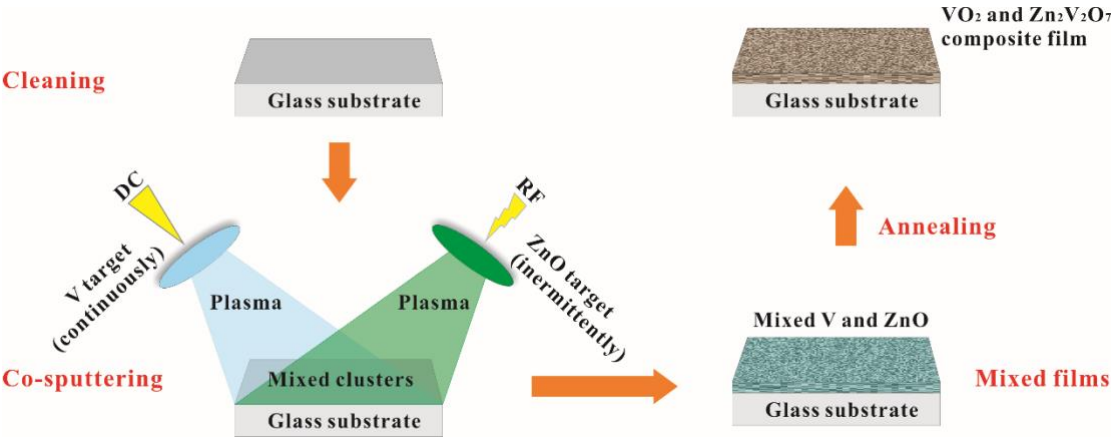

Figure 1. The diagram for fabrication process of VO_2 film and $Zn_2V_2O_7$-VO_2 composite film.

Characterizations. Glancing angel X-ray diffraction (GAXRD) measurement was used to characterize the crystal structure of the film on Empyrean diffractometer (Cu Kα, λ = 0.154178 nm produced under a 4 kW output power). Field emission scanning electron microscopy (FESEM, JSM-5610LV, Japan) was used to observe the morphology of the surface and cross-section of the films. Surface morphology and roughness of films were measured by an atomic force microscopy (AFM, Nanoscope IV/Nanoscope IV, VEECO). X-ray photoelectron spectroscopy (XPS, ESCALAB 250Xi, Thermo Fisher) was employed to characterize the valence of each element in the film. The phase transition temperatures of the films were measured by the vacuum photoconductive tester (VPT). Solar transmittance (300-2500 nm) of films at 20 ºC and 90 ºC respectively was characterized by an ultraviolet-visible-near-infrared spectrophotometer (UV-vis-NIR, UV-3600, SHIMADZU) with an attached temperature control device. The integrated solar modulation efficiency and luminous transmittance of films can be calculated according to formula (1):

$$T_{\mathrm{lum/sol}} = \int \varphi_{\mathrm{lum/sol}}(\lambda)T(\lambda)\mathrm{d}\lambda / \int \varphi_{\mathrm{lum/sol}}(\lambda)\mathrm{d}\lambda \quad (1)$$

where $T(\lambda)$ is the transmittance, λ is the wavelength of the incident light, $\varphi_{\mathrm{lum}}(\lambda)$ denotes the spectral sensitivity of the light to the human eye, and $\varphi_{\mathrm{sol}}(\lambda)$ represents the irradiance spectrum of the sun light at an atmospheric mass of 1.5 (corresponding to the sun from the horizon 37°).[9] ΔT_{sol} can be obtained according to formula (2):

$$\Delta T_{\mathrm{sol}} = T_{\mathrm{sol}}(20\ ^{\circ}\mathrm{C}) - T_{\mathrm{sol}}(90\ ^{\circ}\mathrm{C}) \quad (2)$$

3. RESULTS AND DISCUSSION

Crystal Structure and Morphology of Films. To analyze the crystal structure of the as-prepared composite films, XRD characterization was carried out and the results are shown in Figure 2a. It can be seen, all the diffraction peaks of the VO_2 film match well with the M-phase VO_2 (JCPDS database No. 65-2358), indicating that the prepared film is pure M phase VO_2. For $Zn_2V_2O_7$-VO_2 composite film, some diffraction peaks belong to M-phase VO_2 (JCPDS database No. 65-2358) and other peaks correspond well to $Zn_2V_2O_7$ (JCPDS database No. 28-1497), suggesting that the composite film is composed of VO_2(M) and $Zn_2V_2O_7$. Notably, ZnO was completely reacted with VO_2 to form $Zn_2V_2O_7$ during the annealing process. In addition, most diffraction peaks of the $Zn_2V_2O_7$ film match well with standard $Zn_2V_2O_7$ (JCPDS database No. 28-1497) and a small peak belongs to V_2O_5 (JCPDS database No. 76-1803) in Figure S2a since slight amount of V metal annealing in air condition were directly oxidized into V_2O_5.[32] This indicates that the film is comprised of most $Zn_2V_2O_7$ and a few V_2O_5. The SEM images for surface morphology of these films were shown in Figure 2b and c. It can be seen that these films are composed of fine particles with diameter of about 50-100 nm. Many grain boundaries can also be observed obviously in both films. There are few pores in the $Zn_2V_2O_7$-VO_2 composite film and VO_2 film while no pores in the $Zn_2V_2O_7$ film (Figure S2b). Two-dimensional and three-dimensional atomic force micrographs (Figure 2d and e) exhibit a relative rough surface morphology of the $Zn_2V_2O_7$-VO_2 composite film with root-mean-square roughness (Rq) of 17.1 nm, which might be relate to the composite components with different morphology. It is believed that the rough surface was beneficial to improve luminous transmittance through weakening the specular reflectance.

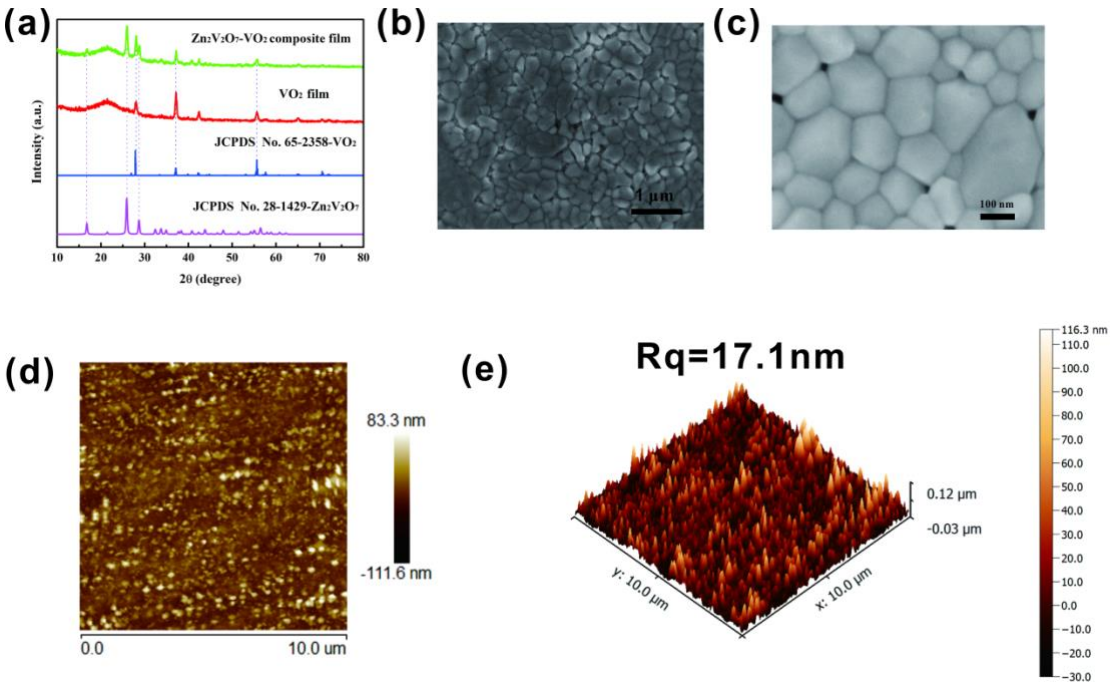

Figure 2. (a) XRD patterns of $Zn_2V_2O_7$-VO_2 composite film and VO_2 film. FESEM images of (b) $Zn_2V_2O_7$-VO_2 composite film, (c) VO_2 film. (d) Two-dimensional and (e) three-dimensional AFM images of the surface morphology for $Zn_2V_2O_7$-VO_2 composite film

Composition Analyses of Films by Means of XPS and EDS. In order to further understand the element composition and the valence of each element in films, XPS characterization was performed and the results were shown in Figure 3. The XPS data were calibrated by standard C1s binding energy of 284.8 eV. V 2p and O 1s peaks were observed in the survey spectra of Figure 3a, confirming the existence of VO_2 in the $Zn_2V_2O_7$-VO_2 composite film and VO_2 film. The Zn 2p peak can be obviously seen in the $Zn_2V_2O_7$-VO_2 composite film but not in pure VO_2 film in Figure 3b revealing the exist of $Zn_2V_2O_7$ combining with XRD results. Furthermore, the Zn 2P core level was split into Zn $2p_{3/2}$ (1022.1 eV) and Zn $2p_{1/2}$ (1045.2 eV) peaks, indicating that there was Zn element with a valence state of +2 in the $Zn_2V_2O_7$-VO_2 composite film. Figure 3c and d show the high-resolution analysis of the V $2p_{3/2}$ and O 1s peaks in VO_2 film as well as their deconvolution analysis based on Gaussian function. V $2p_{3/2}$ can be divided into two peaks of 515.9 eV and 517.2 eV corresponding to the +4 and +5 valences of vanadium, respectively. The presence of V^{5+} ions could be ascribed to partial oxidation of the film exposed in the air.[33-35] The

O 1s of the VO_2 film also corresponded to two peaks at 529.9 eV and 532.1 eV, indicating that two states oxygen in the film indexed to VO_2 and V_2O_5 respectively.[34] In the $Zn_2V_2O_7$-VO_2 composite film, V $2p_{3/2}$ can also be divided into two peaks at 515.5 eV and 517.4 eV, which also corresponded to V^{4+} and V^{5+}, respectively. Quite amount of V^{5+} originated from $Zn_2V_2O_7$ resulting in stronger intensity of V^{5+} core level being achieved in $Zn_2V_2O_7$-VO_2 composite film than that in VO_2 film (Figure 3d).[33,34] The O 1s core level of the composite film with two peaks at 530.3 eV and 531.9 eV were also corresponding to the O elements in VO_2 and $Zn_2V_2O_7$, respectively. This indicates that $Zn_2V_2O_7$ and VO_2 are present in the composite film, which is consistent with the above XRD results.

To further understand the distribution of Zn, V and O in the composite film, elemental mapping analysis were performed on the film surface. The element distribution of V, Zn and O were shown in Figure 4a-c. It can be seen that each element was uniformly distributed in the film, revealing that $Zn_2V_2O_7$ and VO_2 particles adhered together in the composite film. The atomic ratio of V and Zn calculated form the atomic fraction in Figure 4d was about 3.6:1, which was in good agreement with the sputtering time ratio of V target and ZnO target.

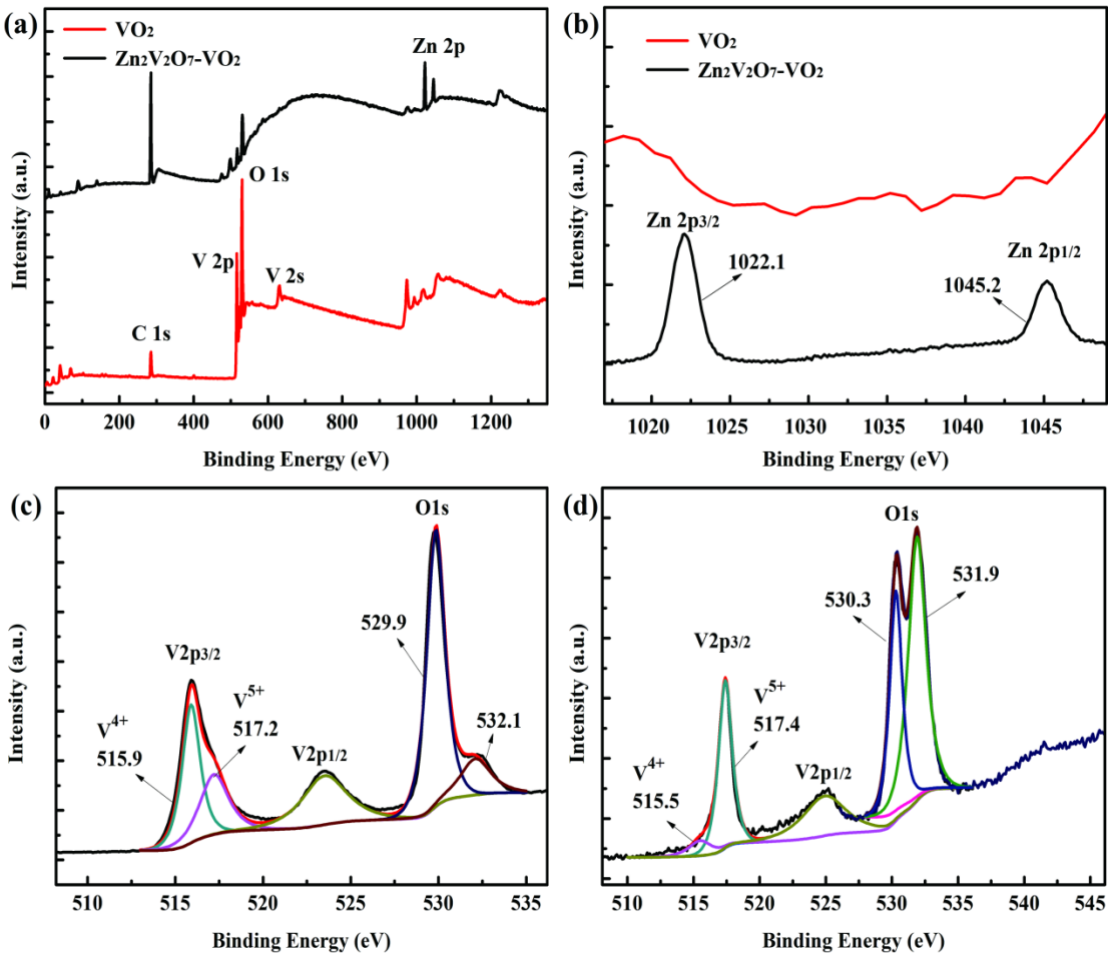

Figure 3. (a) XPS survey spectrum of $Zn_2V_2O_7$-VO_2 composite film and VO_2 film, high-resolution XPS spectrum for (b) Zn 2P, (c) V 2p core level in VO_2 film and (d) O 1s core level in $Zn_2V_2O_7$-VO_2 composite film.

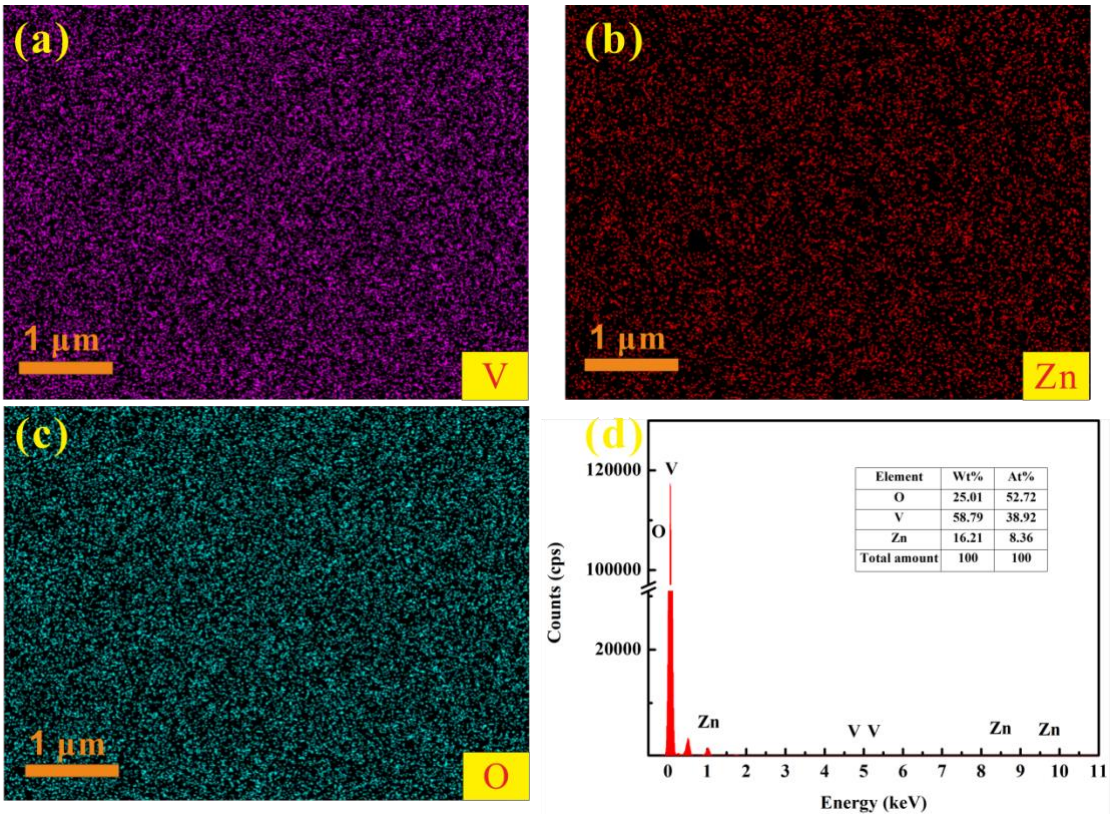

Figure 4. The element mapping for different elements: (a) V, (b) Zn, (c) O of the $Zn_2V_2O_7$-VO_2 composite film and (d) EDS spectrum of corresponding surface (inset is the mass and atomic fraction of V, Zn, O elements).

Thermochromic properties of $Zn_2V_2O_7$-VO_2 composite films. To investigate effect of $Zn_2V_2O_7$ contents on optical properties of $Zn_2V_2O_7$-VO_2 composite films, samples with different ZnO sputtering durations but constant V sputtering time of 16 min were fabricated and the corresponding transmittance were posted in Figure S3. As can be seen, transmittance especially for the visible light region was improved significantly as increasing total ZnO sputtering durations. The specific optical properties were summarized in Table S2, as increasing sputtering duration of ZnO，T_{lum} was increased from 34.1% of VO_2(V) film to 49% of $Zn_2V_2O_7$-VO_2(VZ4) composite film, slight diminish in that of VZ6 film would be contributed to slight film thickness alternation compared with VZ4 since ΔT_{sol} exhibited opposite variation trend. Excessive sputtering duration of ZnO led to synthesis of pure $Zn_2V_2O_7$ (VZ16) film without thermochromic properties evidenced by the superposition of transmittance at 20 ℃ and 90 ℃ (ΔT_{sol}=0) (Figure S2a and Figure S3b). However, it is worth noting that the

$Zn_2V_2O_7$ showed highest T_{lum} of 84%, indicating that $Zn_2V_2O_7$ was an appropriate transparent matrix for improving the optical properties of VO_2 film. Taking the comprehensive optical properties into account, VZ4 ($Zn_2V_2O_7$-VO_2) composite film put up the best performance than others. Therefore, the effect of structures on performance were mainly discussed detailly among VO_2, VZ4 ($Zn_2V_2O_7$-VO_2) and $Zn_2V_2O_7$ films.

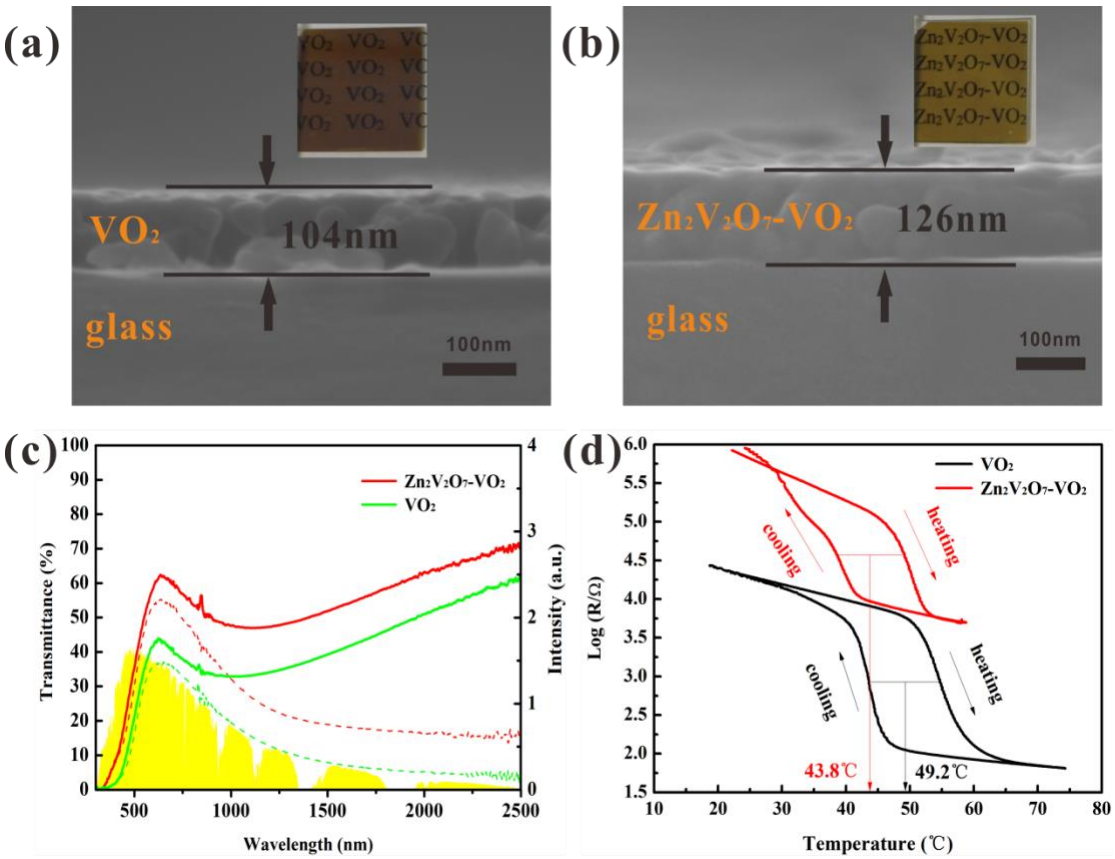

Figure 5. Cross-sectional FESEM images and the optical photographs of (a) VO_2 film, (b) $Zn_2V_2O_7$-VO_2 composite film, (c) optical transmittance spectra in the range from 300 nm to 2500 nm at 20 ℃ (solid lines) and 90 ℃ (dashed lines) and (d) temperature-dependent resistance for $Zn_2V_2O_7$-VO_2 composite film and VO_2 film.

Optical photographs of these films were depicted in Figure 5a, b and Figure S4a. It can be seen that VO_2 film is brown and $Zn_2V_2O_7$ film is pale yellow while the $Zn_2V_2O_7$-VO_2 composite film is brown-yellow that located between color of former two films, further confirming that the composite film is composed of VO_2 and $Zn_2V_2O_7$. In addition, the words under $Zn_2V_2O_7$-VO_2 composite film presented clearer,

indicating that the composite film exhibited a higher luminous transmittance than VO_2 film, and the transmittance spectra presented in Figure 5c ulteriorly demonstrated the deduce aforementioned. Considering that the thickness was an important factor influencing the optical properties of thin films, the film thickness was determined according to the cross-sectional SEM image. Figure 5a, b and Figure S4a compares the representative cross-sectional SEM images of VO_2 film, $Zn_2V_2O_7$-VO_2 composite film and $Zn_2V_2O_7$ film. The thickness depending on the total sputtering durations of V target and ZnO target were 104 nm, 126 nm and 186 nm for VO_2 film, $Zn_2V_2O_7$-VO_2 composite film and $Zn_2V_2O_7$ film, respectively. Even though the thickness was increased by prolonging the total sputtering durations, T_{lum} was enhanced instead. One could explain that the ZnO contents increased in the V-ZnO precursor film react with more VO_2 during annealing, resulting in less VO_2 being preserved in the obtained $Zn_2V_2O_7$-VO_2 composite film compared with pure VO_2 film. Furthermore, generated $Zn_2V_2O_7$ with ultrahigh T_{lum} of 84.0% uniformly dispersed in the $Zn_2V_2O_7$-VO_2 composite film serving as transparent matrix, which was of great importance for enhancement of T_{lum} as well as ΔT_{sol} in accordance with the model of VO_2-SiO_2 composite films (VO_2 nanoparticles dispersed in SiO_2).[36,37] Although ΔT_{sol} was not increased significantly, just from 10.9% for VO_2 film to 11.5% for $Zn_2V_2O_7$-VO_2 composite film. It is impressive to optimize greatly T_{lum} by 43.7% (from 34.1% to 49%) while maintain the ΔT_{sol} slightly being increased (Table 1).[38]

Table 1. Thermochromic properties of VO_2, $Zn_2V_2O_7$-VO_2 and $Zn_2V_2O_7$ films as well as the corresponding optical bandgap.

Samples	T_{lum} (%)	ΔT_{sol} (%)	T_c (℃)	E_g (eV)
VO_2	34.1	10.9	49.2	1.7
$Zn_2V_2O_7$-VO_2	49.0	11.5	43.8	2.8
$Zn_2V_2O_7$	84.0	0	-	3.2

Furthermore, the enhancement in T_{lum} was attributed to the widened optical band gap shown in Figure 6 simultaneously. The optical bandgap was estimated through

transmittance data, by calculating the absorption coefficient α as a function of energy using Beer-Lambert's law as follows.

$$\alpha d = -\ln\frac{T}{1-R} \quad (3)$$

$$(\alpha h\upsilon)^m = A(h\upsilon - E_g) \quad (4)$$

The optical bandgap E_g was derived from equation (4), where the exponent m here was identified as 1/2 for indirect-allowed optical transition. By linear fitting the plot of $(\alpha h\upsilon)^{1/2}$ depend on hυ, E_g was obtained from the intercept of fitted line with x axis (Figure 6) and summarized in Table 1. One can see that optical bandgap become wider as increasing the contents of $Zn_2V_2O_7$. The distinction was quite pronounced that optical bandgap has been widened from 1.7 eV of VO_2 film to 2.8 eV of $Zn_2V_2O_7$-VO_2 composite film. The introduction of $Zn_2V_2O_7$ with higher optical bandgap of 3.2 eV widened optical bandgap and further caused a significant blue shift in the absorption edge, leading to decrease in visible light absorption thus improve luminous transmittance ultimately. Meanwhile, the color of films turned lighter as discussed above.

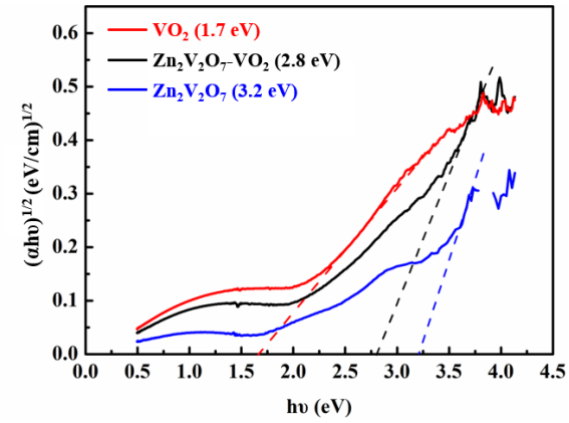

Figure 6. $(\alpha h\upsilon)^{1/2}$ and hυ plots for VO_2, $Zn_2V_2O_7$-VO_2 composite film and $Zn_2V_2O_7$ films, indicating the optical bandgap of each film.

Moreover, the temperature dependent resistance test was carried out on the vacuum photoconductive tester (VPT) and the results were displayed in Figure 5d. The phase transition temperature (T_c) of these films were obtained according to the film temperature dependent resistance curves. Herein, T_c was derived from $T_c=(T_{c,h}+T_{c,c})/2$,

that was, the central point of the hysteresis loop, in which $T_{c,h}$ and $T_{c,c}$ were temperatures where slope is highest in the heating and cooling branches.[39] It can be calculated that $T_{c,h}$ was 49.1 ℃ and $T_{c,c}$ was 38.5 ℃ in $Zn_2V_2O_7$-VO_2 composite film while $T_{c,h}$ was 54.5 ℃ and $T_{c,h}$ was 43.9 ℃ for VO_2 film. In this sense, T_c of $Zn_2V_2O_7$-VO_2 composite film and VO_2 film was 43.8 ℃ and 49.2 ℃ (Table 1), respectively. Obviously, $Zn_2V_2O_7$-VO_2 composite film showed a lower phase transition temperature than that of VO_2 film but much higher resistance than that of VO_2 film at the same temperature. The reduction in the phase transition temperature was probably attributed to the boundaries between $Zn_2V_2O_7$ and VO_2 grains which can cause considerable strain and thus leading to phase transition at lower temperature.[40] The increasement in the film resistance was probably caused by the addition of $Zn_2V_2O_7$ gains with higher resistance than that of VO_2 grains in the composite film. This was confirmed by the temperature dependent resistance curve of $Zn_2V_2O_7$ film in Figure S4c. Therefore, the composite film showed enhanced comprehensive thermochromic performance compared with pristine VO_2 film prepared by magnetron sputtering using V_2O_5 target that with T_{lum} of 36.63% and ΔT_{sol} of 5.87%.[41] To objectively evaluate the thermochromics, a comparison has been made with some best reported works that aiming to improve the thermochromic properties of VO_2 film through microstructures, multilayers and element doping using magnetron sputtering method (Table 2).

As can be seen, Mg, Fe and Si doping have been employed to adjust the thermochromic properties of pristine VO_2 film,[20,42,43] especially, reduce T_c. However, they all failed to improve the optical properties simultaneously, for instance, Mg and Si doping would impair ΔT_{sol} and only reduction of T_c to be found in Fe doping film. Besides, thermochromic properties in this work were more excellent that that of doping films. Double layer structures (VO_2/TiO_2 and Cr_2O_3/VO_2) only affect the optical properties while maintain the T_c of bulk VO_2,[44,45] Furthermore, ZrO_2/$V_{1-x}W_xO_2$/ZrO_2 films aimed to optimize the optical performance as well as decrease T_c through incorporating W into VO_2 lattices.[18,19] Indeed, excellent comprehensive

thermochromic properties with ΔT_{sol} of 49.9%, T_{lum} of 10.4% and T_c of 20 ºC were obtained, but it was quite complicated for designing multilayer structures, and multi-strategies integration would raise the bar of difficult and cost for production. In all, $Zn_2V_2O_7$-VO_2 composite film exhibited comparable overall thermochromic properties compared with that of best reported works.

Table 2. Comparison of thermochromic properties between this work and those best reported VO_2 films fabricated by magnetron sputtering.

System	T_{lum} (%)	ΔT_{sol} (%)	T_c (ºC)	Reference
Mg-doped VO_2 film	~51.0	-	~45.0	20
Fe-doped VO_2 film	36.2	14.6	34.1	42
Si-doped VO_2 film	36.1	9.2	46.1	43
VO_2/TiO_2 film	35.2	10.4	68.0	44
ZrO_2/$V_{0.982}W_{0.018}O_2$/ZrO_2 film	49.9	10.4	20.0	18
ZrO_2/$V_{0.988}W_{0.012}O_2$/ZrO_2 film	42.0	12.0	39.0	19
Cr_2O_3/VO_2 Smart film	46.0	12.2	73.0	45
V_3O_7-V_2O_5-VO_2 Composite film	29.1	20.3	56.7	46
$Zn_2V_2O_7$-VO_2 composite film	**49.0**	**11.5**	**43.8**	This work

"-" means data not mentioned.

4. CONCLUSION

The $Zn_2V_2O_7$-VO_2 composite film was successfully prepared by DC and RF dual-target magnetron co-sputtering and subsequent post-annealing treatment. The $Zn_2V_2O_7$-VO_2 composite film showed improved luminous transmittance (T_{lum}=49.0%), suitable solar modulation efficiency (ΔT_{sol}=11.5%) and lower phase transition temperature (T_c=43.8 ℃) than pristine VO_2 film. The enhancement in the thermochromic performance was probably attributed to the addition of $Zn_2V_2O_7$ grains in the composite film which can consume some VO_2 grains to form $Zn_2V_2O_7$-VO_2 interface. The uniform distribution of $Zn_2V_2O_7$ grains in the composite film can increase the visible transmittance since $Zn_2V_2O_7$ can strongly widen the

optical bandgap of $Zn_2V_2O_7$-VO_2 film. The $Zn_2V_2O_7$-VO_2 grain boundaries will produce considerable strain to trigger the phase transition at lower temperature. The composite film overcomes the primary weaknesses of the pure VO_2 films prepared by magnetron sputtering for smart windows and thus becomes a promising material to create energy-saving devices in the future. In addition, this work opens the door to future studies of interface-dependent behavior in composite film, as well as possible integration into other devices.

ASSOCIATED CONTENT

Supporting Information

Preparation details of $Zn_2V_2O_7$-VO_2 composite films with different ZnO sputtering durations; XRD pattern and surface SEM image of $Zn_2V_2O_7$ film; transmittance at 20 ℃ and 90 ℃ and calculated optical properties (T_{lum} and ΔT_{sol}) of films with various total sputtering durations for ZnO target; cross-section SEM image, transmittance at 20 ℃ and 90 ℃ and temperature-dependent resistance of $Zn_2V_2O_7$ film.

AUTHOR INFORMATION

Corresponding Authors

*E-mail address: tiansq@whut.edu.cn (S. Tian).

*E-mail address: lineng@whut.edu.cn (N. Li).

ORCID

ACKNOWLEDGMENTS

This work was supported by the National Natural Science Foundation of China (Grant No. 51772229 and 52062045), the 111 project (No. B18038), the National Key R&D Program of China (No. 2017YFE0192600), Key R&D Project of Hubei Province (No.2020BAB061), Open Research Fund Program of Science and Technology on Aerospace Chemical Power Laboratory (No. STACPL220191B02), National innovation and entrepreneurship training program for college students (No.

201910497034), Open Foundation of the State Key Laboratory of Silicate Materials for Architectures at WUT (No. SYSJJ2020-04), State Key Laboratory of Materials Processing and Die & Mould Technology, Huazhong University of Science and Technology (No. P2021-010) and the Fundamental Research Funds for the Central Universities (No. 195201024). We also thank the Analytical and Testing Center of WUT for the help with carrying out XRD, TEM, and FESEM analyses.

REFERENCES

(1) Houška, J.; Kolenatý, D.; Vlček, J.; Cerstvy, R.; Properties of Thermochromic VO_2 Films Prepared by HiPIMS onto Unbiased Amorphous Glass Substrates at A Low Temperature of 300 °C. *Thin Solid Films* **2018**, *660*, 463-470.

(2) Babulanam, S. M.; Eriksson, T. S.; Niklasson, G. A. Thermochromic VO_2 Films for Energy-Efficient Windows. *Sol. Energ. Mater.* **1987**, *16*, 347-363.

(3) Gorgolis, G.; Karamanis, D. Solar Energy Materials for Glazing Technologies. *Sol. Energ. Mater. Sol. C.* **2016**, *144*, 559-578.

(4) Morin, F. J. Oxides Which Show A Metal-to-insulator Transition at the Neel Temperature. *Phys. Rev. Lett.* **1959**, *3*, 34-36.

(5) Zhu, M.; Qi, H.; Wang, B.; Wang, H.; Guan, T.; Zhang, D. Thermochromism of Vanadium Dioxide Films Controlled by the Thickness of ZnO Buffer Layer under Low Substrate Temperature. *J. Alloy. Compd.* **2018**, *740*, 844-851.

(6) Du, J.; Gao, Y. F.; Chen, Z.; Kang, L. T.; Zhang, Z. T.; Luo, H.J. Enhancing Thermochromic Performance of VO_2 Films via Increased Microroughness by Phase Separation. *Sol. Energ. Mater. Sol. C.* **2013**, *110*, 1-7.

(7) Ji, Y. X.; Li, S. Y.; Niklasson, G. A.; Granqvist, C. G. Durability of Thermochromic VO_2 Thin Films under Heating and Humidity: Effect of Al Oxide Top Coatings. *Thin Solid Films* **2014**, *562*, 568-573.

(8) Orlianges, J. C.; Crunteanu, J. Leroy, A.; Mayet, R. Electrical and Optical Properties of Vanadium Dioxide Containing Gold Nanoparticles Deposited by Pulsed Laser Deposition. *Appl. Phys. Lett.* **2012**, *101*, 133102.

(9) Li, B.; Tian, S. Q.; Tao, H. Z.; Zhao, X. J. Tungsten Doped M-phase VO_2 Mesoporous Nanocrystals with Enhanced Comprehensive Thermochromic Properties for Smart Windows. *Ceram. Int.* **2019**, *4*, 4342-4350.

(10) Leroy, J.; Bessaudou, A.; Cosset, F.; Crunteanu, A. Structural, Electrical and Optical Properties of Thermochromic VO_2 Thin Films Obtained by Reactive Electron Beam Evaporation. *Thin Solid Films* **2012**, *520*, 4823-4825.

(11) Vernardou, D.; Paterakis, P.; Drosos, H.; Spanakis, E.; Poveyim, I. M.; Pemble,

M. E.; Koudoumas, E.; Katsarakis, N. A Study of the Electrochemical Performance of Vanadium Oxide Thin Films Grown by Atmospheric Pressure Chemical Vapour Deposition. *Sol. Energ. Mater. Sol. C.* **2011**, *95*, 2842-2847.

(12) Suh, J. Y.; Lopez, R.; Feldman, L. C.; Haglun, R. F. Semiconductor to Metal Phase Transition in the Nucleation and Growth of VO_2 Nanoparticles and Thin Films. *J. Appl. Phys*. **2004**, *96*, 1209-1213.

(13) Koo, H.; Xu, L.; Ko, K.E.; Ahn, S.; Chang, S. H.; Park, C. Effect of Oxide Buffer Layer on the Thermochromic Properties of VO_2 Thin Films. *J. Mater. Eng. Perform.* **2013**, *22*, 3967-3973.

(14) Gagaoudakis, E.; Michail, G.; Aperathitis, E.; Kortidis, I.; Binas, V.; Panagopoulou, M.; Raptis, Y. S.; Tsoukalas, D.; Kiriakidis, G. Low-temperature rf Sputtered VO_2 Thin Films as Thermochromic Coatings for Smart Glazing Systems. *Adv. Mater. Lett.* **2017**, *8*, 757-761.

(15) Cavalleri, A.; Rini, M.; Chong, H. H. W.; Fourmaux, S.; Glover, T. E.; Heimann, P. A.; Kieffer, J. C.; Schoenlein, R. W. Band-Selective Measurements of Electron Dynamics in VO_2 Using Femtosecond Near-Edge X-Ray Absorption. *Phys. Rev. Lett.* **2005**, *95*, 067405.

(16) Zhu, M.; Shan, C.; Li, C.; Wang, H.; Qi, H.; Zhang, D.; Lv, W. Thermochromic and Femtosecond-Laser-Induced Damage Performance of Tungsten-Doped Vanadium Dioxide Films Prepared Using an Alloy Target. *Materials* **2018**, *11*, 1724.

(17) Ji, C.; Wu, Z.; Wu, X.; Feng, H.; Wang, J.; Huang, Z.; Zhou, H.; Yao, W.; Gou, J.; Jiang, Y. Optimization of Metal-to-Insulator Phase Transition Properties in Polycrystalline VO_2 Films for Terahertz Modulation Applications by Doping. *J. Mater. Chem. C* **2018**, *6*, 1722-1730.

(18) Kolenatý, D.; Vlček, J.; Bárta, T.; Rezek, J.; Houška, J.; Haviar, S.; High-performance thermochromic VO_2-based coatings with a low transition temperature deposited on glass by a scalable technique. *Sci. Rep.* **2020**, *10*, 1-12.

(19) Houška, J.; Kolenatý, D.; Vlček, J.; Bárta, T.; Rezek, J.; Cerstvy, R.; Significant improvement of the performance of $ZrO_2/V_{1-x}W_xO_2/ZrO_2$ thermochromic

coatings by utilizing a second-order interference. *Sol. Energy. Mat. Sol. C.* **2019**, *191*, 365-371.

(20) Mlyuka, N. R.; Niklasson, G. A.; Granqvist, C. G. Mg Doping of Thermochromic VO_2 Films Enhances the Optical Transmittance and Decreases the Metal-Insulator Transition Temperature. *Appl. Phys. Lett.* **2009**, *95*, 291.

(21) Batista, C.; Ribeiro, R. M.; Teixeira, V. Synthesis and Characterization of VO_2-Based Thermochromic Thin Films for Energy-Efficient Windows. *Nanoscale Res. Lett.* **2011**, *6*, 301.

(22) Jiang, M.; Cao, X.; Bao, S.; Zhou, H.; Jin, P. Regulation of the Phase Transition Temperature of VO_2 Thin Films Deposited by Reactive Magnetron Sputtering without Doping. *Thin Solid Films* **2014**, *562*, 314-318.

(23) Xu, H. Y.; Huang, Y. H.; Liu, S.; Xu, K. W.; Ma, F.; Chu, P. K. Effects of Annealing Ambient on Oxygen Vacancies and Phase Transition Temperature of VO_2 Thin Films. *RSC Adv.* **2016**, *6*, 79383-79388.

(24) Kolenaty, D.; Houska, J.; Vlcek, J. Improved Performance of Thermochromic VO_2/SiO_2 Coatings Prepared by Low-temperature Pulsed Reactive Magnetron Sputtering: Prediction and Experimental Verification. *J. Alloy. Compd.* **2018**, *767*, 46-51.

(25) Zhu, M.; Qi, H.; Wang, B.; Wang, H.; Zhang, D.; Lv, W. Enhanced Visible Transmittance and Reduced Transition Temperature for VO_2 Thin Films Modulated by Index-tunable SiO_2 Anti-reflection Coatings. *RSC Adv.* **2018**, *8*, 28953-28959.

(26) Zhou, H.; Li, J.; Bao, S.; Li, J.; Liu, X.; Jin, P. Use of ZnO as Antireflective, Protective, Antibacterial, and Biocompatible Multifunction Nanolayer of Thermochromic VO_2 Nanofilm for Intelligent Windows. *Appl. Surf. Sci.* **2016**, *363*, 532-542.

(27) Chu, X.; Tao, H.; Liu, Y.; Ni, J.; Bao,J.; Zhao, X. VO_2/AZO Double-layer Films with Thermochromism and Low-emissivity for Smart Window Applications. *J. Non-Cryst. Solids* **2014**, *383*, 121-125.

(28) Mlyuka, N. R.; Niklasson, G. A.; Granqvist, C. G. Thermochromic Multilayer Films of VO_2 and TiO_2 with Enhanced Transmittance. *Sol. Energ. Mater. Sol. C.* **2009**,

93, 1685-1687.

(29) Zheng, J.; Bao, S.; Jin, P. TiO_2(R)/VO_2(M)/TiO_2(A) Multilayer Film as Smart Window: Combination of Energy-saving, Antifogging and Self-cleaning Functions, *Nano Energy* **2015**, *11*, 136-145.

(30) Sameie, H.; Sabbagh Alvani, A. A.; Naseri, N.; Du, S.; Rosei, F. First-Principles Study on ZnV_2O_6 and $Zn_2V_2O_7$: Two New Photoanode Candidates for Photoelectrochemical Water Oxidation. *Ceram. Int.* **2018**, *44*, 6607-6613.

(31) Sato, K.; Hoshino, H.; Mian, M. S.; Okimura, K. Low-temperature Growth of VO_2 Films on Transparent ZnO/glass and Al-doped ZnO/glass and Their Optical Transition Properties. *Thin Solid Films* **2018**, *651*, 91-96.

(32) Julien, C.; Haro-Poniatowski, E.; Camacho-López, M. A.; Escobar-Alarcón, L.; Jímenez-Jarquín, J. Growth of V_2O_5 Thin Films by Pulsed Laser Deposition and Their Applications in Lithium Microbatteries. *Mater. Sci. Eng. B.* **1999**, *65*, 170-176.

(33) Liang, S.; Shi, Q.; Zhu, H.; Peng, B.; Huang, W. One-Step Hydrothermal Synthesis of W-Doped VO_2 (M) Nanorods with a Tunable Phase-Transition Temperature for Infrared Smart Windows. *ACS Omega* **2016**, *1*, 1139-1148.

(34) Chiu, T. W.; Hong, R. T.; Tonooka, K.; Kikuchi, N. Microstructure of Orientation Controlled VO_2 Thin Films via ZnO Buffer. *Thin Solid Films* **2013**, *529*, 119-122.

(35) Wu, S.; Tian, S.; Liu, B.; Tao, H.; Zhao, X.; Palgrave, R.G.; Sankar, G.; Parkin, I. P. Facile Synthesis of Mesoporous VO_2 Nanocrystals by a Cotton-template Method and Their Enhanced Thermochromic Properties. *Sol. Energ. Mater. Sol. C.* **2018**, *176*, 427-434.

(36) Schläefer, J.; Sol, C.; Li, T.; Malarde, D.; Portnoi, M.; Macdonald, T. J.; Laney, S. K.; Powell, M. J.; Top, I; Parkin, I. P. Papakonstantinou, I.; Thermochromic VO_2-SiO_2 nanocomposite smart window coatings with narrow phase transition hysteresis and transition gradient width. *Sol. Energ. Mater. Sol. C.* **2019**, *200*, 109944.

(37) Qu, Z.; Yao, L.; Ma, S.; Li, J.; He, J. H.; Mi, J.; Tang, S. Y.; Feng, L. Rational design of HSNs/VO_2 bilayer coatings with optimized optical performances and mechanical robustness for smart windows. *Sol. Energ. Mater. Sol. C.* **2019**, *200*,

109920.

(38) Kang, L.; Gao, Y.; Luo, H.; Wang, J.; Zhu, B.; Zhang, Z.; Du, J.; Kanehira, M.; Zhang, Y. Thermochromic Properties and Low Emissivity of ZnO:Al/VO_2 Double-Layered Films with A Lowered Phase Transition Temperature. *Sol. Energ. Mater. Sol. C.* **2011**, *95*, 3189-3194.

(39) Long, S.; Cao X.; Huang, R.; Xu, F.; Li, N.; Huang, A.; Sun, G.; Bao, S.; Luo, H.; Jin, P. Self-Template Synthesis of Nanoporous VO_2-Based Films: Localized Surface Plasmon Resonance and Enhanced Optical Performance for Solar Glazing Application, *ACS Appl. Mater. Interfaces* **2019**, *11*, 22692−22702

(40) Li, X.; Schaak, Raymond E. Size-and Interface-Modulated Metal-Insulator Transition in Solution-synthesized Nanoscale VO_2-TiO_2-VO_2 Heterostructures. *Angew. Chem.* 2**017**, *129*, 15756-15760**.**

(41) Ho, H.-C.; Lai, Y.-C.; Chen, K.; Dao, T. D.; Hsueh, C.-H.; Nagao, T. High Quality Thermochromic VO_2 Films Prepared by Magnetron Sputtering Using V_2O_5 Target with in situ Annealing. *Appl. Surf. Sci.* **2019**, *495*, 143436.

(42) Lu, L.; Wu, Z. M.; Ji, C. H.; Song, M. Z.; Feng, H. Q.; Ma, X. T.; Jiang, Y. D. Effect of Fe doping on thermochromic properties of VO_2 films. *J. Mater. Sci-Mater. El.* **2018**, *29*, 5501-5508.

(43) Wu, X. F.; Wu, Z. M.; Zhang, H. F.; Niu, R. H.; He, Q.; Ji, C. H.; Wang, J.; Jiang, Y. D. Enhancement of VO_2 thermochromic properties by Si doping. *Surf. Coat. Tech.* **2015**, *276*, 248-253.

(44) Juan, P.-C.; Lin, K.-C.; Lin, C.-L.; Tsai, C.-A.; Chen, Y.-C. Low Thermal Budget Annealing for Thermochromic VO_2 Thin Films Prepared by High Power Impulse Magnetron Sputtering. *Thin Solid Films* **2019**, *687*, 137443.

(45) Chang, T. C.; Cao, X.; Li, N.; Long, S. W.; Gao, X. .; Dedon, L. R.; Sun, G. Y.; Luo, H. J.; Jin, P. Facile and low-temperature fabrication of thermochromic Cr_2O_3/VO_2 smart coatings: enhanced solar modulation ability, high luminous transmittance and UV-shielding function. *ACS Appl. Mater. Inter.* **2017**, *9*, 26029-26037.

(46) Gu, D.; Li, Y. T.; Zhou, X.; Xu, Y. Facile fabrication of composite vanadium

oxide thin films with enhanced thermochromic properties. *ACS Appl. Mater. Inter.* **2019**, *11*, 37617-37625.